Supplement of Biogeosciences, 23, 8407–8420, 2026
https://doi.org/10.5194/bg-23-8407-2026-supplement
© Author(s) 2026. CC BY 4.0 License.



Biogeosciences Open Access EGU

Supplement of

Disentangling the biotic and abiotic drivers of evapotranspiration in a degraded raised bog

Vincent E. Flemming et al.

Correspondence to: Vincent E. Flemming (vincent.flemming@uni-muenster.de)

The copyright of individual parts of the supplement might differ from the article licence.

Supplementary Material

S1 The effect of gap-filled data on the driver analysis of daily LE

We analysed canopy conductance and drivers of LE on daily flux estimates. However, in Eddy Covariance measurements, portions of the daily data are filtered during quality control. To obtain unbiased daily values, these gaps must be filled using interpolation, regression, or machine learning approaches. Such gap-filling procedures, however, impose a relationship between the predictors and the target variable.

Restricting analyses to observed data alone is impractical at the daily scale, as most days contain filtered measurements due to turbulence-based quality control. In our dataset, only 178 days of the three years were completely free of gap-filled data. Importantly, only 12% of daily aggregates required more than 60% gap-filling, thus observed values largely dominate the daily totals.

To test the influence of modeled datapoints on our results we repeated the analysis with five different thresholds of 10%, 25%, 50%, 75% and 100% of maximum daily gap-filled datapoints allowed. During each run all other datapoints were removed from the dataset.

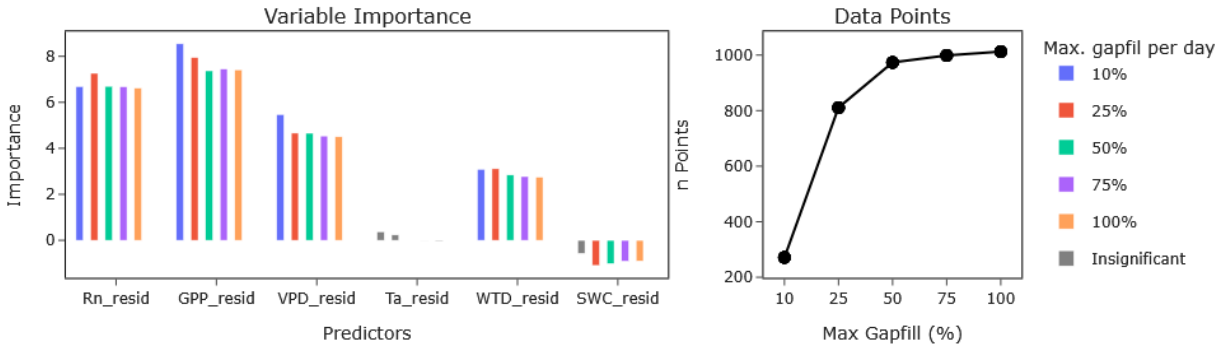


Figure S1: Left: Predictor importances for different imposed maximum allowed percentages of filled data per day. Grey bars indicate insignificance of the predictor. Right: Number of datapoints included when imposing the thresholds of maximum modeled data per day

Across all thresholds of allowed maximum daily gap-filled data we found that the driver importances are very similar (Fig. S1). We saw an increase in the importance of VPD and GPP and a small increase in the importance of WTD at a threshold of 25% or lower, however that did not affect the relative ranking of the drivers in any case. Residuals of SWC became insignificant at a threshold of 10%, however imposing such a strict threshold leaves only 24% of the data and is likely to introduce bias, due to the differences in mean missing datapoints per day between the months (Fig. S2). While the average missing datapoints per day are highest in July due to two larger gaps in the data, across the other months the average missing data is highest in January, February and December, resulting in higher data loss in winter compared to summer when filtering data on gap-filling thresholds.

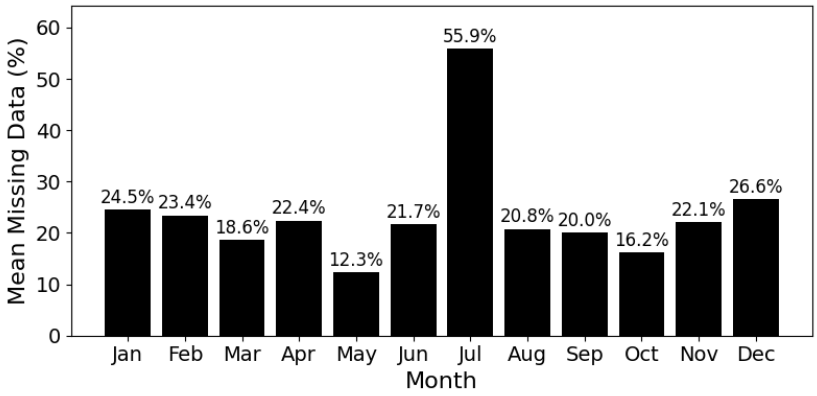


Figure S2: Mean missing datapoints per day in each month.

Summarizing, while there is minor variation in the driver's importance when limiting the amount of filled data to very strict thresholds, the driver rankings and magnitudes remain mostly stable across the full range, until the threshold is so strict that an un-skewed sampling within the year cannot be guaranteed.

S2 Start and end of growing seasons

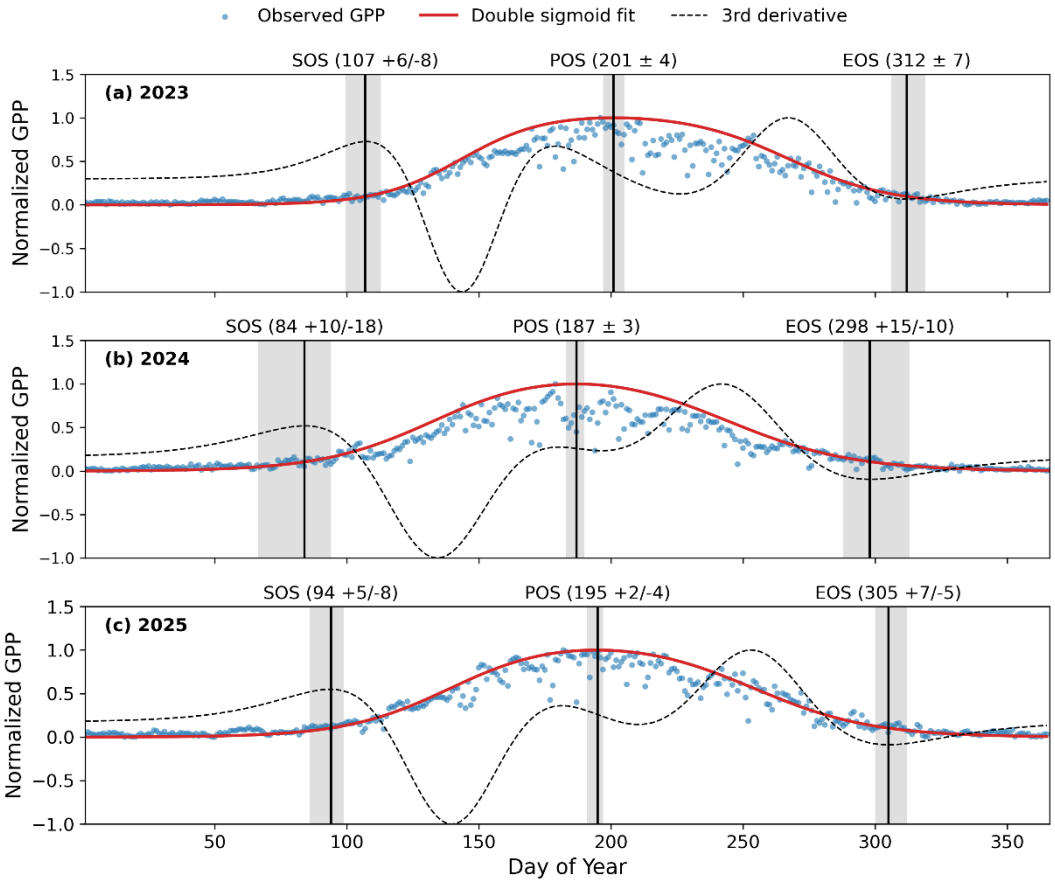


Figure S3: Start (SOS), peak (POS), and end (EOS) of the growing season for the years 2023 (a), 2024 (b), and 2025 (c). The x-axis shows the Day of Year, and the y-axis shows normalized gross primary production (GPP, blue dots) in DE-Amv. The vertical black lines show the Day of Year for SOS, POS, and EOS, and the gray area shows the corresponding 95% confidence intervals. To calculate the confidence intervals, the analysis was repeated multiple times using subsamples of GPP. The red line shows the double sigmoid function fitted to GPP, and the dashed line shows the third derivative of the function.

S3 Measurement devices

Table S1: Included variables, measuring devices used and unit of the variables.

Variable	Device	Unit
H_2O	LI7200RS gas analyzer	μmol s^{-1} m^{-2}
wind speed, wind direction	Gill HS50 sonic anemometer	m s^{-1}, °
air temperature (T_a)	Vaisala HMP155	°C
relative humidity (rH)	Vaisala HMP155	%
radiation (R)	Kipp&Zonen CNR4	W m^{-2}
(–5 cm) soil temperature (T_s)	Soil T. Thermistor 7900-180	°C
(–5 cm) soil heat flux (SHF)	Hukseflux HFP10SC	W m^{-2}
(–5 cm) soil water content (SWC)	Stevens Hydraprobe	m^3 m^{-3}
precipitation (P)	TR-525M	mm
water table depth (WTD)	RXMOD-W1	cm

S4 Bowen ratio

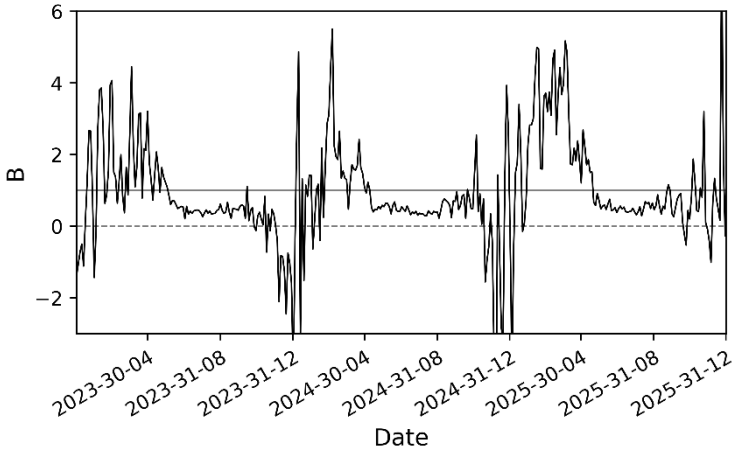


Figure S4: Bowen ratio (B) for the measurement period (1 January 2023 to 31 December 2025): The values are aggregated to three-day values.

S5 Stability of change point with different rates of transpiration contributing to evapotranspiration

To examine how the calculated change point in the relationship between canopy conductance (g_c) and vapor pressure deficit (VPD), or g_c and soil water content (SWC), changes as the proportion of transpiration (T) relative to evapotranspiration (ET) varies, the calculation of g_c was repeated using different T/ET ratios. For the change point involving VPD, the result remains stable at 7.6 hPa for T/ET ratios between 0.8 and 1, is 7.3 hPa for T/ET ratios between 0.6 and 0.7, and is 7.2 hPa for a T/ET ratio of 0.5 (Fig. S5a). The change point for T/ET ratios between 0.5 and 1 remains stable at 0.62 for SWC (Fig. S5b).

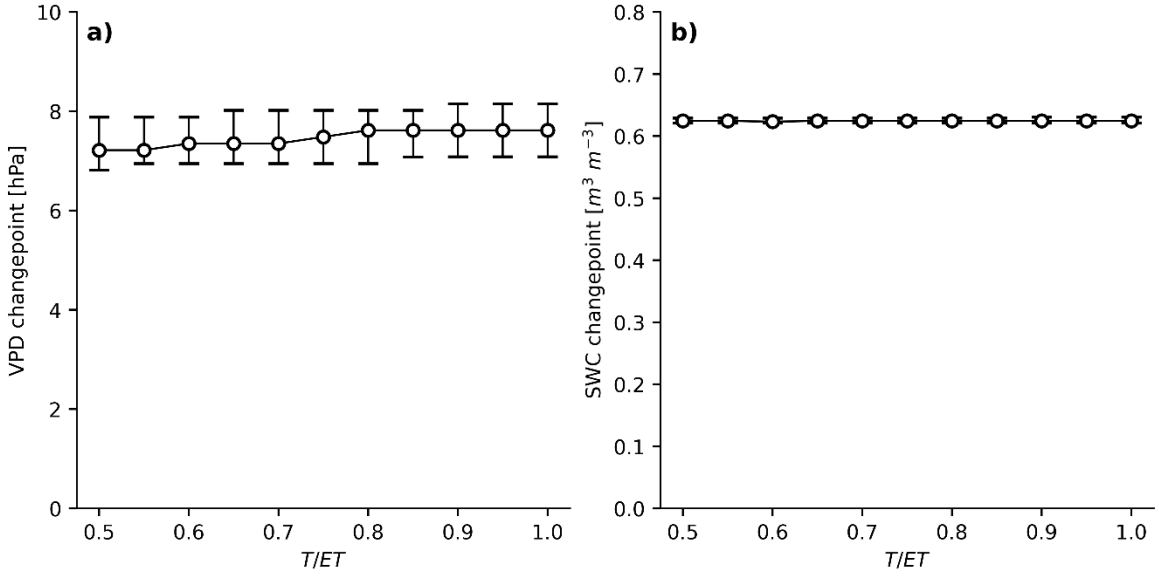


Figure S5: Stability test of the change points for the relationships between a) canopy conductance (g_c) and vapor pressure deficit (VPD) and b) g_c and soil water content (SWC). The proportion of transpiration (T) relative to evapotranspiration (ET) is shown on the y-axis. Vertical lines show the 95% confidence interval for the change points obtained using bootstrapping (n=1000).

In addition, we partitioned ET into T and evaporation (E) using several methods, implemented in the Python package "partitioning" by Zahn (2024). The following ET partitioning methods were used: conditional eddy covariance (CEC) (Zahn et al., 2022), modified relaxed eddy accumulation (Thomas et al., 2008), flux-variance similarity (FVS) (Scanlon et al., 2019; Scanlon and Sahu, 2008), conditional eddy accumulation (Zahn et al., 2024), and CEC with water use efficiency (Zahn et al., 2024).

ET partitioning showed significantly different results across methods, with the median value being T/ET = 0.79 (Fig. S6). Due to the low consistency of ET partitioning results across methods, ET was used instead of T to calculate canopy conductance (g_c). As a test, in addition to filtering by time of day and periods without interception, filtering was performed using FVS (constant ratio), retaining only those ET values for which the T_{FVS}/ET_{FVS} ratio was greater than or equal to 0.8. FVS was chosen because, in a comparison of partitioning models, it produced the most accurate results and, in particular, exhibited the most uniform error (Zahn et al., 2024). The thresholds for g_c with increasing VPD and SWC remained unchanged by the T/ET filter;

accordingly, this additional filter was not applied to the actual analysis, and consequently, no further parts of the data were removed.

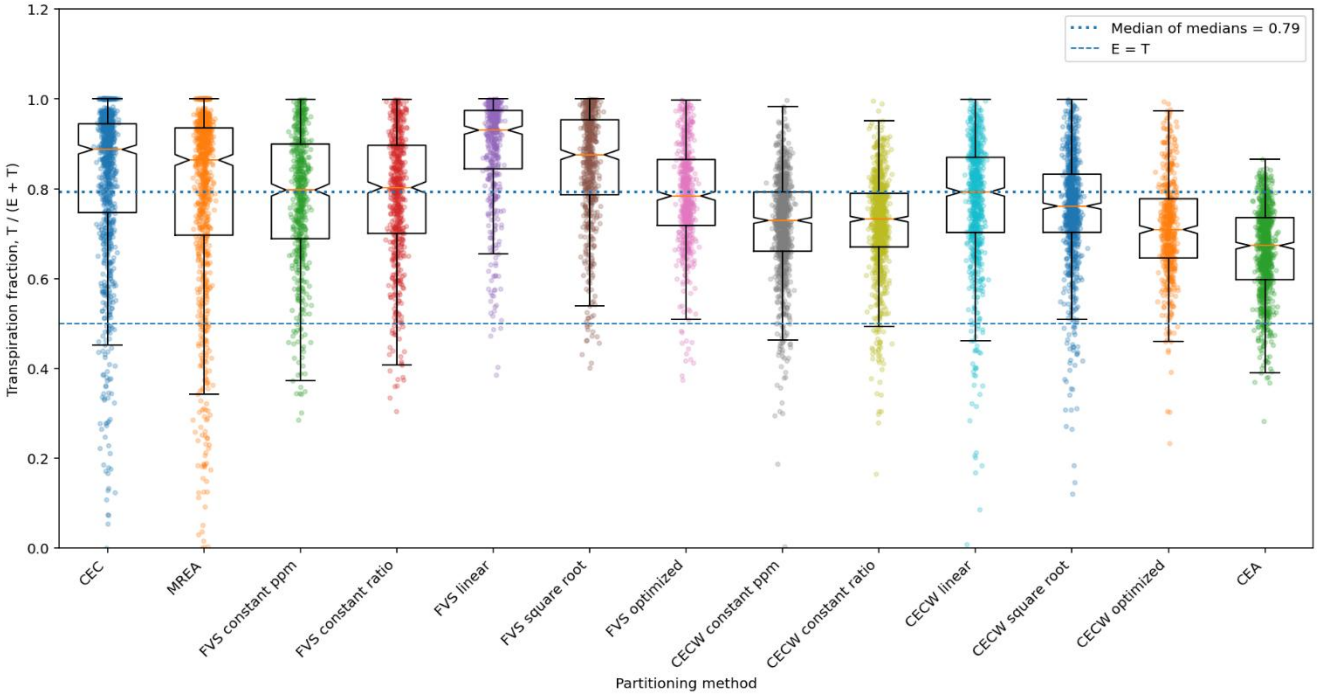


Figure S6: Ratio of transpiration (T) to evapotranspiration (ET). Each box plot represents an ET partitioning method: CEC = conditional eddy covariance, MREA = modified relaxed-eddy accumulation, FVS = flux-variance similarity, CECW = CEC with water use efficiency (WUE), and CEA. FVS and CECW both require WUE, which was calculated using the following methods: constant ppm, constant ratio, linear, square root, and optimized.

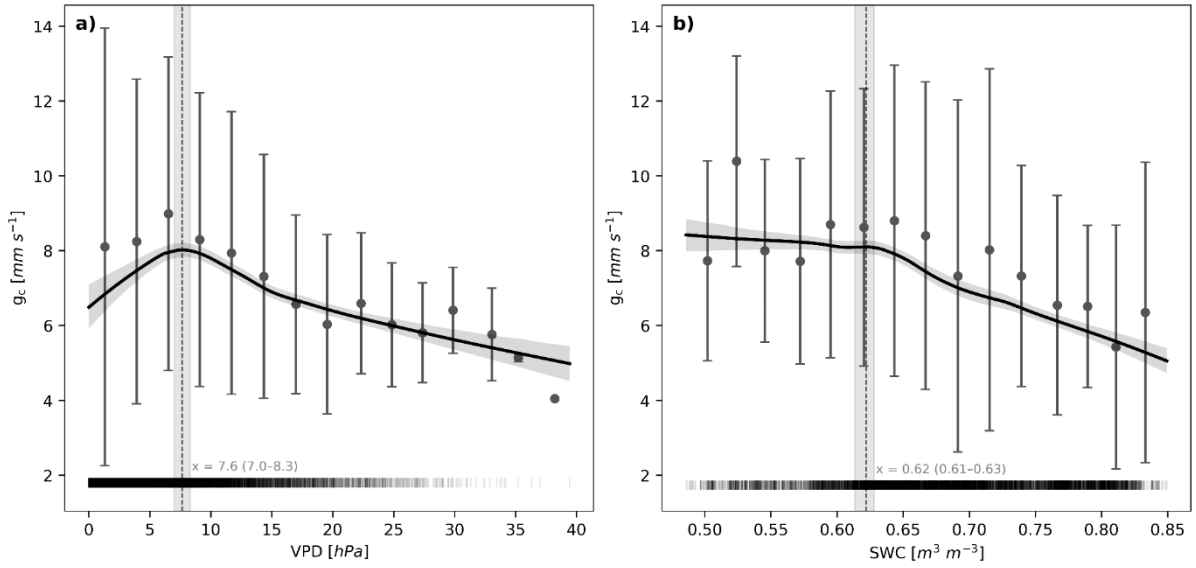


Figure S7: Relationship between a) canopy conductance (g_c) and vapor pressure deficit (VPD) and b) g_c and soil water content (SWC). The data have a resolution of 30-minutes and were calculated using equation 2. Vertical lines in gray show mean and standard deviation for bins of the individual data points, in black a local polynomial regression. Gray area shows the 95% confidence interval of the regression and its rightmost local maximum obtained using bootstrapping (n=1000). The vertical dashed line indicates the rightmost local maximum of the regression line. The lines on the x-axis show the data distribution. Data were restricted to the growing seasons and between 8h and 16h. Different from Figure 6, the data here was additionally filtered for T/ET ≥ 0.8 using T and ET from FVS (constant ratio) partitioning.

References

Scanlon, T.M., Sahu, P., 2008. On the correlation structure of water vapor and carbon dioxide in the atmospheric surface layer: A basis for flux partitioning. Water Resources Research 44 (10).

Scanlon, T.M., Schmidt, D.F., Skaggs, T.H., 2019. Correlation-based flux partitioning of water vapor and carbon dioxide fluxes: Method simplification and estimation of canopy water use efficiency. Agricultural and Forest Meteorology 279, 107732.

Thomas, C., Martin, J.G., Goeckede, M., Siqueira, M.B., Foken, T., Law, B.E., Loescher, H.W., Katul, G., 2008. Estimating daytime subcanopy respiration from conditional sampling methods applied to multi-scalar high frequency turbulence time series. Agricultural and Forest Meteorology 148 (8-9), 1210–1229.

Zahn, E., 2024. PartitioningMethods. https://github.com/einaraz/PartitioningMethods. Accessed 18 September 2026.

Zahn, E., Bou-Zeid, E., Good, S.P., Katul, G.G., Thomas, C.K., Ghannam, K., Smith, J.A., Chamecki, M., Dias, N.L., Fuentes, J.D., Alfieri, J.G., Kwon, H., Caylor, K.K., Gao, Z., Soderberg, K., Bambach, N.E., Hipps, L.E., Prueger, J.H., Kustas, W.P., 2022. Direct partitioning of eddy-covariance water and carbon dioxide fluxes into ground and plant components. Agricultural and Forest Meteorology 315, 108790.

Zahn, E., Ghannam, K., Chamecki, M., Moene, A.F., Kustas, W.P., Good, S., Bou-Zeid, E., 2024. Numerical Investigation of Observational Flux Partitioning Methods for Water Vapor and Carbon Dioxide. J. Geophys. Res. 129 (6).